university of groningen

University Medical Center Groningen

University of Groningen

Non-Interceptive Beam Current and Position Monitors for a Cyclotron Based Proton Therapy Facility

Srinivasan, Sudharsan

DOI:
10.33612/diss.149817352

IMPORTANT NOTE: You are advised to consult the publisher's version (publisher's PDF) if you wish to cite from it. Please check the document version below.

Document Version
Publisher's PDF, also known as Version of record

Publication date:
2021

Link to publication in University of Groningen/UMCG research database

Citation for published version (APA):
Srinivasan, S. (2021). *Non-Interceptive Beam Current and Position Monitors for a Cyclotron Based Proton Therapy Facility*. [Thesis fully internal (DIV), University of Groningen]. University of Groningen. https://doi.org/10.33612/diss.149817352

Copyright
Other than for strictly personal use, it is not permitted to download or to forward/distribute the text or part of it without the consent of the author(s) and/or copyright holder(s), unless the work is under an open content license (like Creative Commons).

The publication may also be distributed here under the terms of Article 25fa of the Dutch Copyright Act, indicated by the “Taverne” license. More information can be found on the University of Groningen website: https://www.rug.nl/library/open-access/self-archiving-pure/taverne-amendment.

Take-down policy
If you believe that this document breaches copyright please contact us providing details, and we will remove access to the work immediately and investigate your claim.

Downloaded from the University of Groningen/UMCG research database (Pure): http://www.rug.nl/research/portal. For technical reasons the number of authors shown on this cover page is limited to 10 maximum.

Download date: 20-04-2025

Chapter 4: Design of a Four-quadrant Dielectric-filled Reentrant Cavity Resonator as a Proton Beam Position Monitor (BPM) Using HFSS Simulation

This Chapter and the next Chapter are combined in the following paper, which is under submission for a peer-reviewed journal.

S. Srinivasan, P-A. Duperrex, J. M. Schippers, S. Brandenburg, Development of a Four-quadrant Dielectric-filled Reentrant Cavity as a Beam Position Monitor (BPM) for Proton Radiation Therapy Facility at Paul Scherrer Institute (PSI)

4.1 Introduction

In Chapter 2 and Chapter 3, we designed and characterized the beamline performance of a non-invasive beam current monitor based on the excitation of the monopole (TM_{010}) mode resonance in a reentrant coaxial cavity. These results provided the motivation to investigate the feasibility of a resonant cavity as a beam position monitor (BPM). However, a TM_{010} mode excited cavity does not provide any position information as discussed in Chapter 2 and experimentally demonstrated in Chapter 3. Therefore, the excitation of other electromagnetic (EM) modes has been investigated.

Beam position measurements are based on transducers that are sensitive to the beam position with respect to them by detecting the electromagnetic fields induced by the beam. The distortion of these fields depends on the beam position, which allows for accurate beam position measurement [1]. To measure the beam position with a good resolution, the beam current is an important baseline parameter, as it determines the signal-to-noise ratio (SNR).

For PROSCAN, the small beam-induced signals for beam currents in the range 0.1-10 nA limit the sensitivity of conventional non-invasive BPMs such as capacitive pickups and Wall Current Monitors (WCMs). Hence, at PROSCAN,

beam position information is measured by interceptive techniques such as multi-strip ionization chambers (ICs) and secondary emission monitors [2]. The downside of using these monitors is that they affect the beam properties due to multiple scattering. In order to get rid of these scattering effects, a non-interceptive beam position monitor is considered for the PROSCAN beamlines.

An off-centered beam will excite a dipole mode (TM_{110}) excitation in a resonant cavity [3]. Therefore, it could be a good candidate for non-interceptive beam position measurements. Cavity resonators excited in the TM_{110} mode directly provide a signal amplitude per unit of displacement [3] for off-centered beams only. The position information from a resonant cavity with a TM_{110} mode excitation is directly available as discussed in Chapter 1. In comparison to other non-interceptive monitors, in which the position information is generally provided by the difference between signals of two opposing pickups, the cavity resonator proposed here does not require the subtraction of signals to derive position information. In this Chapter, we investigate the TM_{110} mode excitation in a reentrant cavity as a potential candidate to measure beam position at the low beam currents in PROSCAN.

At PROSCAN, the COMET cyclotron delivers a proton beam in bunches with a repetition rate of 72.85 MHz. The cavity is designed such that the resonance frequency of theTM_{110} mode in the reentrant cavity resonator is at 145.7 MHz, which is the second harmonic of the beam bunch repetition rate. This frequency is chosen for reasons already discussed in Chapter 2.

4.1.1 Dipole mode (TM_{110}) cavity characterization

Prior to designing a TM_{110} mode cavity for monitoring beam positions, it is important to have a general overview of the TM_{110} mode and to have an analytical estimate of the pickup signal for a given position offset of the beam. The detailed description of the theoretical background used in this section can be found in [3]–[6].

Here, the characterization of a TM_{110} mode cavity is explained from the perspective of a generic pillbox cavity. The TM_{110} mode, a transverse magnetic mode, is antisymmetric and its amplitude is linearly dependent on the gap radius of a conventional pillbox cavity [5]. The TM_{110} mode, represented in cylindrical coordinates (r,ϕ,z) where r is the radial distance, ϕ is the azimuth angle, z is the longitudinal distance) has no longitudinal magnetic field component ($B_z=0$) and a non-vanishing longitudinal electric field component ($E_z\neq0$). The excited TM_{110}

mode in any resonator is defined by the cavity geometry. For a simple pillbox cavity design, the cavity radius R_{res} and the gap length l define the cavity geometry as shown in Figure 4.1. The TM_{110} mode is represented in cylindrical coordinates (r,ϕ,z) with the indices m, n, p (TM_{mnp}) as defined in ref. [4]

- (m=1) One full period sinusoidal variation of the field components along the azimuthal direction. In cylindrical resonators:
  $E, B \propto \cos(m\phi)$ or $\sin(m\phi)$
- (n=1) One zero crossing of the longitudinal field components in the radial direction. In cylindrical resonators: $E_z, B_z \propto J_m(a_{mn}\delta x/R_{res})$ where, a_{mn} are zeros of J_m, the Bessel functions of the first kind. δx is the beam position offset with respect to the central axis and R_{res} is the radius of the cylindrical resonator
- (p=0) zero half-period sinusoidal variation of the field components in the longitudinal direction. In cylindrical resonators:
  $E, B \propto \cos(p\pi z/l)\ or\ \sin(p\pi z/l)$. l is the gap length in the cylindrical resonator

The resonance frequency of such a mode is given by [6]

$$\omega_{mnp} = \frac{1}{\sqrt{\mu_o \varepsilon_o}} \sqrt{\left(a_{mn}/R_{res}\right)^2 + \left(p\pi/l\right)^2},$$

$$\omega_{110} = \frac{1}{\sqrt{\mu_o \varepsilon_o}} \frac{a_{11}}{R_{res}}, \tag{4.1}$$

The fields of the TM_{110} mode, ignoring the effects of coupling ports and beam pipe, are given by [5], [7],

$$\left|E_{z,110}\right| = C_{110} J_1\left(\frac{a_{11}\delta x}{R_{res}}\right)\cos\phi \tag{4.2}$$

$$H_{r,110} = -i\, C_{110} \frac{\omega_{110}\varepsilon_o R_{res}^{\ 2}}{a_{11}^2 \delta x} J_1\left(\frac{a_{11}\delta x}{R_{res}}\right)\sin\phi e^{i\omega_{110}t} \tag{4.3}$$

$$H_{\phi,110} = -i\, C_{110} \frac{\omega_{110}\varepsilon_o R_{res}}{a_{11}} J_1'\left(\frac{a_{11}\delta x}{R_{res}}\right)\cos\phi e^{i\omega_{110}t} \tag{4.4}$$

where C_{110} represents the amplitude of the oscillation.

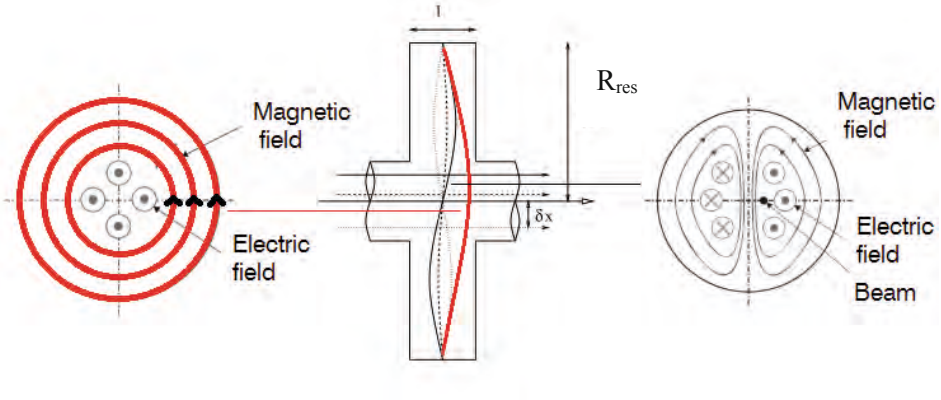

Figure 4.1: Schematic representation of the induced TM_{010} (red field lines) and TM_{110} modes (black field lines) in a generic cylindrical cavity (pillbox). The magnetic field amplitude of an offset beam is shown in the central figure. An offset beam excites both modes. The TM_{110} mode amplitude is proportional to both beam current and offset. The TM_{010} mode amplitude is proportional only to beam current. Same offset but in the opposite direction induces the same signal but with opposite phase (continuous and dotted lines) [5].

According to the fundamental theorem of beam loading [8], an acceleration a charged particle gets while passing an empty cavity is exactly one-half of its own induced voltage. The energy stored in a mode within the cavity then can be expressed as

$$W_{mnp} = \frac{1}{2}\varepsilon_o \int_V \left|E_{z,mnp}\right|^2 dV \tag{4.5}$$

The voltage along the longitudinal direction of the particle beam in a cavity at the TM_{110} mode is represented as [9]

$$V_{110} = 2\, q\, k_{110} \text{ with } k_{110} = \frac{V_{110}^2}{4\, W_{110}} = \frac{\omega_{110}}{2}\left(\frac{R}{Q_o}\right)_{110} \tag{4.6}$$

where, q is the bunch charge in Coulombs; k_{110} is the loss factor of the TM_{110} mode in V/C and ω_{110} is the angular TM_{110} resonance frequency. R is the shunt impedance for TM_{110} mode and as per circuit theory, its expression can be found in [3]. Q_0 is the unloaded Quality factor of the TM_{110} mode within a cavity (cavity walls: σ is conductivity, μ is permeability) given by

$$Q_o = \frac{1}{2\pi}\frac{a_{11}}{1+\frac{R_{res}}{l}}\frac{\lambda_{110}}{\delta} \text{ where, } \delta \text{ is the skin-depth} \tag{4.7}$$

The quantity $(R/Q_0)_{110}$ is the normalized shunt impedance of the TM_{110} mode and its expression at the location of the maximum electric field ($\delta x = 0.48R$) in a generic pillbox is given by

$$\left(\frac{R}{Q_o}\right)_{110} = \frac{2\,Z_0\,l\,(J_1^{max})^2\,T_{tr}^2}{\pi\,R_{res}\,J_o^2(a_{11})\,a_{11}} \approx 130.73\,\frac{l}{R_{res}}\,T_{tr}^2 \tag{4.8}$$

where $a_{11} = 3.83$ is the first zero of J_1; $J_1^{max} = 0.582$ the maximum of the first-order Bessel function; $J_o(a_{11}) = 0.402$ is the root (solution) of the zero-order Bessel function that corresponds to the first zero of the first-order Bessel function. $Z_o = 377\ \Omega$ is the free-space characteristic impedance. The location of the maximum electric field is given by the ratio of the location where the maximum of the first-order Bessel function is, to the location of the first zero of the same Bessel function. T_{tr}, the transit-time factor, is the maximum energy gained in the cavity normalized to the cavity voltage [10] and is as given in [11] for low energy beams.

The voltage induced in the TM_{110} mode by a charge q for a given position offset δx can be evaluated by taking the line integral of Eq (4.2) along the particle trajectory. The induced voltage for any arbitrary offset can then be expressed as

$$V_{110}^{in}/V_{110}^{max} = J_1(a_{11}\delta x)/J_1^{max},\ V_{110}^{in} = \frac{2k_{110}\,q\,a_{11}\,\delta x}{2J_1^{max}\,R_{res}} \tag{4.9}$$

The Bessel function $J_1(x)$ can be replaced by x/2 for small offsets, so the voltage becomes linearly proportional to δx (the error of this approximation is less than 1% for δx up to 15% of R_{res}). Substituting Eq (4.6) and (4.8), in the above equation, provides us the general expression of induced voltage for a given offset δx

$$V_{110}^{in}(\delta x) = \omega_{110}\,q\left(\frac{R}{Q_o}\right)_{110}\left\langle\frac{a_{11}\,\delta x}{2J_1^{max}\,R_{res}}\right\rangle = \frac{0.2474\,\delta x\,q\,l\,T_{tr}^2}{R_{res}^3} \tag{4.10}$$

where, q is expressed in pC and l in m. The voltage coupled out from the cavity into a 50 Ω measuring system can then be expressed as

$$V_{110}^{out}(\delta x) = \left(\frac{R}{Q_o}\right)_{110}\omega_{110}\,q\sqrt{\frac{50\Omega}{Q_L}}B_c\frac{\chi}{1+\chi} = V_{110}^{in}(\delta x)\left(\left(\frac{R}{Q_0}\right)_{110}\right)^{-0.5}\sqrt{\frac{50\Omega}{Q_L}}\sqrt{1-\frac{Q_L}{Q_0}} \tag{4.11}$$

where, χ is the pickup coupling coefficient given by $\chi=Q_o/Q_{ext}$. Q_{ext} can be calculated from subsection 2.1.3. B_c is the beam coupling coefficient and is equivalent to the angle bracket term in Eq (4.10).

4.2 Design Considerations

4.2.1 TM_{110} mode polarization

In Figure 4.1, it can be seen that both the TM_{110} mode and the TM_{010} mode are excited at $r \neq 0$. Since we are interested in the TM_{110} mode, it is important to minimize the amplitude of other modes (especially TM_{010} mode) at the resonance frequency of the TM_{110} mode. This can be achieved by having a high quality factor of the TM_{010} mode and a large resonance frequency separation between the TM_{010} and the TM_{110} modes. However, by opting for a strong coupling due to the demand to measure position information for low beam currents (0.1-10 nA), the quality factor of these modes would be lowered, which will result in an increased amplitude of the TM_{010} mode at the TM_{110} mode frequency.

The TM_{110} mode is a combination of both horizontal and vertical polarization for an arbitrary beam position (X, Y) as represented in Figure 4.2. For a pure X offset (i.e., Y = 0), the vertical polarization is not excited and is vice-versa.

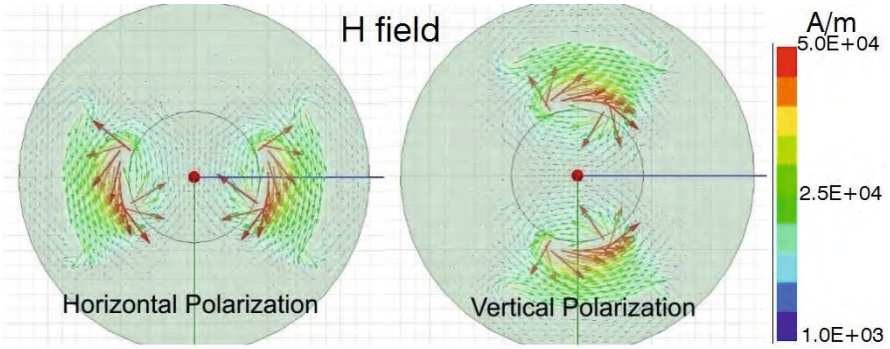

Figure 4.2: TM_{110} mode as a combination of horizontal and vertical polarization. Plotted are the $\vec{H}$ vectors from the Eigenmode solution of the BPM prototype as a non-coupled model (No pickup ports).

For a beam offset in a cavity, as shown in Figure 4.3, the total field strength is a combination of both the TM_{010} and the TM_{110} mode amplitudes [12]. At the left side of the cavity, these mode amplitudes add up vectorially, while at the right side, they subtract. This changes with the beam offset in the opposite direction. However, as can be seen in Figure 4.1, the amplitude of the TM_{110} signal only

gives the magnitude of the beam offset, but not the sign (direction) of the displacement. Subtracting Left and Right signals will zero the TM_{010} mode and double the amplitude of the TM_{110} mode for a given beam offset. When the TM_{010} mode presence at the TM_{110} mode frequency is minimized, the amplitudes of the L and R signals are hardly affected by the TM_{010} contribution. In this case, a separate reference cavity, whose TM_{010} mode frequency is the same as the TM_{110} mode position cavity, should be placed at a known distance before the TM_{110} mode position cavity to determine the sign of the beam displacement. The sign of displacement is then decided by the phase of the L and R signals with respect to the phase of the signal from that separate TM_{010} mode cavity [13].

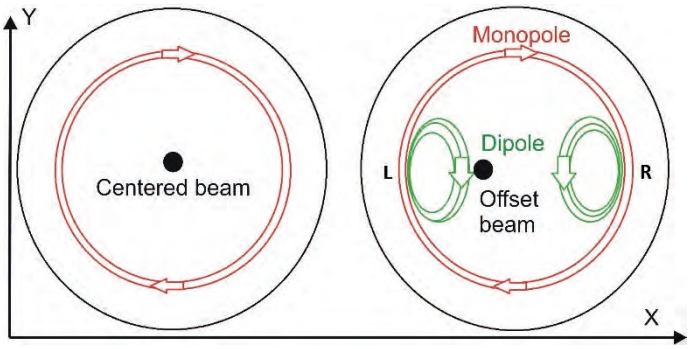

Figure 4.3: B field representation of the TM_{010} and TM_{110} modes of a generic cylindrical geometry. The left image has no TM_{110} mode for a centered beam. The right image shows the additional existence of TM_{110} mode with its polarities for an offset position in the X-axis.

However, it is important to note, that in our case, such a separate reference TM_{010} mode cavity might not be necessary to determine the sign of the beam offset. This is because we expect that the vectorial superposition of the TM_{010} and TM_{110} modes will help to determine the sign of the beam offset, as shown in Figure 4.3.

4.2.2 Choice of Cavity type: Pillbox vs Dielectric-filled Reentrant

In this cavity BPM design, the TM_{110} mode resonance frequency is fixed at the second harmonic of the beam repetition rate. At this frequency, RF interference from the cyclotron RF cavities is minimized and the beam signal amplitude for excitation of the TM_{110} mode is larger than other higher harmonics. The choices of design for the BPM cavity are limited by space constraints in the PROSCAN beamline as already discussed in Chapter 3. For a pillbox design, the radius of the pillbox cavity would be approximately 1.27 meters by substituting a_{11}=3.83 in Eq (4.1). A dielectric-filled reentrant cavity, on the other hand, is much more

compact than a pillbox for the same resonance frequency, as we have seen in Chapter 2.

The fundamental idea for mechanical simplicity is to have a common dielectric in the reentrant gap of the four floating cavities, suspended within a common grounded cylinder. Such a design is expected to save on the required volume at the expense of more complex mechanical design and potentially mode interference due to the necessity to couple more signal power from the cavity. It could also have limitations because of stray field coupling between the floating cavities, i.e., mutual pickup coupling and the coupling of the individual cavities with the ground cylinder. The mutual pickup coupling (crosstalk) could affect the measurement sensitivity as it is expected to be the dominant stray field coupling term that affects the TM_{110} mode.

With a stronger beam coupling coefficient, we expect to couple out more power, which will result in a lower loaded quality factor. As a consequence, the dielectric-filled BPM cavity is expected to have a higher output voltage for a given beam current, compared to a conventional pillbox cavity as per Eq (4.11). This is due to the fact that the normalized shunt impedance is higher for a reentrant cavity system than for a pillbox cavity as per Eq (4.8).

4.2.3 Choice of Coupling: Magnetic

Beam position information can be coupled out of the cavity either by probing the H-field or by probing the E-field. Coupling out information with a simple pickup (as either a loop or an antenna) has the drawback of coupling out all excited modes simultaneously. Using an intrinsic design such as a slot or a waveguide [9] that acts as a high-pass filter can help in minimizing the signal contributions at other frequency components. However, for our scenario, this is not possible due to space constraints. Thus, we keep the choice of coupling as a loop in the inductive region of the cavity BPM similar to the large pickups in the BCM design. With this choice of coupling, it would be possible to determine the amplitude contributions from both the modes by measuring the phase of the cavity signal with respect to the cyclotron RF in contribution with a model that provides information on the phase difference between the TM_{010} and the TM_{110} modes for a given position offset.

4.2.4 Choice of materials and dimension limitations

Regarding the dielectric, the material of choice is not macor as used in the BCM. Since macor is a relatively high loss dielectric, the unloaded quality factor of the

TM_{110} mode in a reentrant cavity BPM with macor would be low, resulting in low signal amplitude. Since the amplitude of the TM_{110} mode within a cavity is close to the cavity center generally weaker than that of the TM_{010} mode, the priority is to keep the unloaded quality factor of the TM_{110} mode as high as possible. This will result in a larger amplitude of the TM_{110} mode excitation within the cavity for a given beam current and thus give a higher amplitude of the signal coupled out of the cavity. However, this demands the stability of the TM_{110} mode resonance frequency under temperature variations, external vibrations, etc. To realise a high quality factor, 99.5% aluminum oxide [14] is chosen as dielectric (ε_r=9.8 and loss factor given by $\delta \leq 0.0001$). This ensures minimum power loss in the dielectric unlike in the BCM. Polyether ether ketone (PEEK) (ε_r=3.0, $\delta \leq 0.003$) will be used to suspend the floating cavities within the ground cylinder to ensure there is no electrical contact between them. This is an important design feature, which keeps the overall system compact for the 145.7 MHz resonance frequency. A conductive (metallic) contact between all the floating cavities would be equivalent to a single dielectric-filled cavity realization within a ground cylinder whose TM_{110} mode signal amplitude for a given position offset would be expected to be lower compared to the floating cavity design as verified with the simulation.

The choice of material for the BPM prototype is aluminum and its relevant material properties are listed in Table 2.1. The same design limitations as considered for the cavity BCM in Chapter 2 applies to the design of the cavity BPM. The dimensions are limited to 45 mm (beam pipe radius) for the inner radius of the alumina ring and the inner radius of the inner coaxial cylinder (floating cavity). The inner radius of the outer coaxial cylinder (of the floating cavity) is limited to 90 mm. Tuning the other dimensions of the BPM system to obtain the TM_{110} mode resonance frequency of 145.7 MHz has been done with the help of Eigenmode and Driven Modal solvers of ANSYS HFSS. The next section describes the evolution of BPM design through parametric investigation of cavity, dielectric, support materials, and pickup position.

4.3 ANSYS HFSS simulations

The ANSYS HFSS uses two solvers to evaluate the dimensional parameters of the BPM that corresponds to the design TM_{110} resonance frequency of 145.7 MHz. The two solvers are:

- Eigenmode to evaluate Eigenmode frequencies of the BPM, the unloaded quality factors, and fields associated with it. The criterium for the

simulation convergence is the frequency difference with respect to the 145.7 MHz frequency of the second harmonic of the cyclotron RF frequency. Convergence criteria is $\Delta\text{Frequency} \leq 0.01\%$.

- Driven modal solver to determine the S-parameter coupling coefficients such that it has maximum beam-pickup coupling coefficients and minimum mutual pickup coupling coefficients. The optimal design dimensions are evaluated from Driven solutions. The criterium for simulation convergence is the change in S_{ji} from one iteration to the next given as $\Delta|S_{ji}| \leq 0.02$ dB.

4.3.1 Eigenmode Solution Setup

The Eigenmode solution setup is used to determine certain fundamental design parameters of the cavity BPM. As mentioned earlier, the BPM is evolved from the cavity BCM design described in Chapter 2. Four LC cavities are suspended within a common grounded cylinder. Two cavities are mounted in the horizontal and two cavities in the vertical plane to probe the X-plane and Y-plane TM_{110} modes, respectively.

The curved surface area of the common grounded cylinder volume is assigned with the conductivity of aluminum. The properties of the other boundaries are directly determined by HFSS by assigning a material type for individual cavities (aluminum), the common dielectric (alumina ceramic), and the supporting PEEK. 180° degree mirror symmetries were imposed on the model in the simulation. The accuracy of calculation is determined by the convergence criteria in the Eigenmode solver.

The Eigenmode solution setup is summarized in Table 4.1.

Table 4.1: Summary of the solution setup model indicating some of the fundamental design parameters. d – inner diameter of inner coaxial cylinder and diameter of beam pipe, C – outer diameter of the alumina ring, t – dielectric thickness, W – inner diameter of the ground cylinder, D – inner diameter of the outer coaxial cylinder, p – PEEK (support ceramic) thickness (diameter = 20mm), alumina width =28mm. All floating cavities are separated by 40mm with respect to each other.

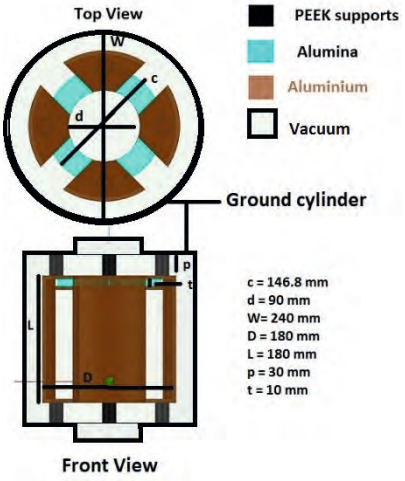

Materials	**Vacuum, Alumina, Aluminum**	
Boundaries	Aluminum finite conductivity on curved surfaces of the ground cylinder	
Excitation	None for Eigenmode	
Mesh Operations	Curvilinear, Skin-depth on Tau mesher	
Analysis	Minimum Frequency	100 MHz
	No. of Modes	4
	No. of passes	20
	Convergence, Δf	0.01%
	Initial Mesh	λ refinement
	Refinement per pass	20%
	Order of Basis functions (solutions)	2^{nd} order
Results	E, H plots, Resonance Frequencies, Q_o	

Results

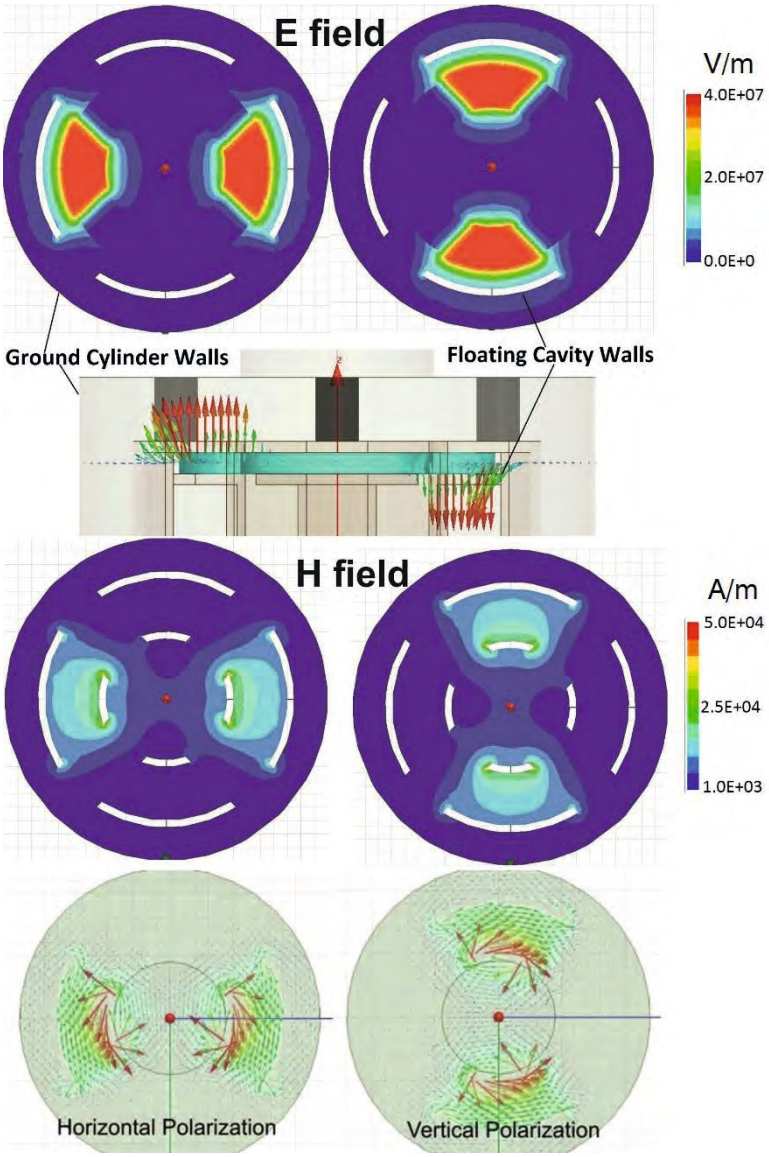

Figure 4.4: E and H fields (magnitude and vector) of the TM_{110} mode (both horizontal and vertical polarization) excited within the cavity. The field plots are extracted from the Eigenmode solver of HFSS. E field is plotted in the center plane of the dielectric. H field is plotted at a plane 30 mm above the base of the floating cavities. The outer line represents the conducting surface of the outer grounded cylinder. The edges where the field terminates represent the conducting surface (boundary termination) of the floating cavities. The TM_{110} mode is localized within the floating cavities.

The Eigenmode solution provides the fundamental dimensional parameters of the BPM prototype such that the TM_{110} mode resonance is matched to the design frequency of 145.7 MHz. Moreover, the Eigenmode solution provides information on the unloaded quality factor (Q_o). Since the TM_{110} mode is a combination of both horizontal and vertical polarization, the Eigenmode solution finds the TM_{110} mode resonance frequency of 145.7 MHz (along with Q_o) for each of the polarization. The unloaded quality factors for both polarization are Q_o = 3158 (H); 3163 (V) with their resonance frequencies as f_{110} = 145.06 MHz (H); 145.08 MHz (V). The small differences in the values are indicative of the accuracy achieved in the simulation. An important observation is the influence of the alumina in the reentrant gap. In the absence of the alumina, the TM_{110} mode resonance frequency of the model is approximately at 274.7 MHz and the unloaded quality factor is 4200. The alumina in the reentrant gap brings the resonance frequency down to approximately 145 MHz while the unloaded quality factor is reduced to 3160. Macor in the reentrant gap would have reduced the unloaded quality factor by approximately 95% from Q_o = 3160 to 267. This clearly indicates that alumina is an almost loss-free dielectric as compared to macor. The presence of PEEK as a support material also does not influence the quality factor of the TM_{110} mode drastically (1% higher without PEEK supports). This important feature is confirmed by the Eigenmode solution. The induced fields of the non-coupled BPM cavity is shown in Figure 4.4 (both magnitude and vector).

The Eigenmode solutions are exported to the Driven modal setup to perform fine-tuning of the resonator by taking into consideration the influence of the inductive pickups and the beam analogon acting as the drive signal, which is modeled as a sinewave in a perfect electric conductor.

4.3.2 Driven modal Solution Setup

The Eigenmode solver provides the solutions of the unloaded cavity BPM design (without beam pipe extensions and pickup ports). However, we need pickup ports to extract the induced field that contains information on the beam position. The Driven modal solution setup helps to characterize the BPM by quantifying the RF energy propagation within a multiport network taking into consideration the beam pipe extensions and the pickup ports. The solutions of the Driven modal are represented as S_{ji} (Scattering parameters) being either transmission or reflection coefficients. As mentioned in Chapter 2, the Driven modal solver helps to analyze

the BPM in the presence of a beam analog such as a stretched wire of narrow cross-sectional area that is defined as a perfect electric conductor.

The signal-coupling scheme is similar to the BCM in Chapter 2. For an inductive loop, the output signal is given as the surface integral of the scalar product of $\vec{H}$ and loop area, as already described in Chapter 2. The BPM is equipped with four loops, one for each floating cavity. Unlike the BCM, the BPM is designed with all four loops having the same size. Since each loop is a measurement port, the possibility to use a resonance trombone for tuning purposes is not available in the BPM. This places a strict limit on the dimensional tolerances of the individual floating cavities, the dielectric and the measurement loops.

Parametric Model

As described in Chapter 2, the model from the Eigenmode solver is imported into the Driven modal setup. The fundamental parameters mentioned in subsection 4.3.1 are transferred as parameters to investigate their role in exciting the TM_{110} mode at the design frequency of 145.7 MHz. Moreover, the parametric investigation provides insight into the prospects of modifying the performance of the cavity BPM by altering the loaded quality factor, improving signal sensitivity, minimizing TM_{010} mode presence, minimizing stray capacitances, etc.

The definitions of boundary conditions and the excitations are given in Chapter 2.

Analysis setup

We summarize the analysis setup in Table 4.2. The Driven modal analysis is performed for two different cases; with a beam analog to optimize dimensions and without a beam analog for the optimized design to evaluate XY isolation, i.e., crosstalk and TM_{110} mode coupling, i.e., XX/YY isolation. The description of how the solver provides the solution by adaptively converging has already been described in Chapter 2.

Table 4.2: Driven modal solution setup (solver conditions) and frequency sweep conditions to solve the model and extract S-parameters

Driven Modal Analysis setup	
Solution Frequency	145.7 MHz
Maximum No of passes (Adaptive)	20
Maximum ΔS (Adaptive)	0.02 dB
Initial mesh options	λ refinement
Maximum Refinement per pass (Adaptive)	20%
Order of Basis functions	2nd
Maximum ΔZ_o	2%
Frequency Sweep (Fast sweep with 0.1 MHz step size)	130-161.4 MHz (with beam analog) & 10-510 MHz (without beam analog)
Optimized parameters	Gap between the cavities, Gap between the ground cylinder and the cavities, Ceramic width, Ceramic thickness, Pickup position

The parametric investigation of certain parameters mentioned in Table 4.2 will be presented in the following subsection. These parameters were considered to tune the TM_{110} mode resonance frequency as well as to optimize the signal output from the measurement ports. According to Eq (4.1), we can tune the resonance frequency by modifying the radius of the resonator. Using Eqs (4.10) and (4.11), we can maximize the signal output for a given bunch charge and offset by:

- Increasing normalized shunt impedance, $(R/Q_0)_{,110}$, by reducing the effective gap radius (through the inter-cavity gap or dielectric width) and increasing the gap height (dielectric thickness).
- Increasing beam coupling coefficient, B_c, by reducing effective gap radius (through the inter-cavity gap or dielectric width).
- The Q_L, (i.e., loaded quality factor) can be influenced by the pickup position, the inter-cavity gap or the intra-cavity gap.

Parametric investigation results

The parametric investigations provide insight into the impact of certain dimensions on cavity characteristics and extracted signal strengths. All parametric investigations are performed with a beam analog offset of 2 mm. Ports 1 and 2 represent the beam entrance and exit ports, which are normalized on their characteristic impedance to minimize reflections within the model. Ports 3 to 6 are measurement ports terminated with 50 Ω impedance. A sketch of the simulation setup is represented in Figure 4.5. We investigated the effect of the following parameters on the TM_{010} and the TM_{110} mode resonance frequencies, their loaded quality factors, and the signal sensitivity for a given position offset:

- Gap between individual cavities (Inter-cavity gap)
- Gap between Cavities and Grounded cylinder (Intra-cavity gap)
- Dielectric width and thickness
- Pickup position

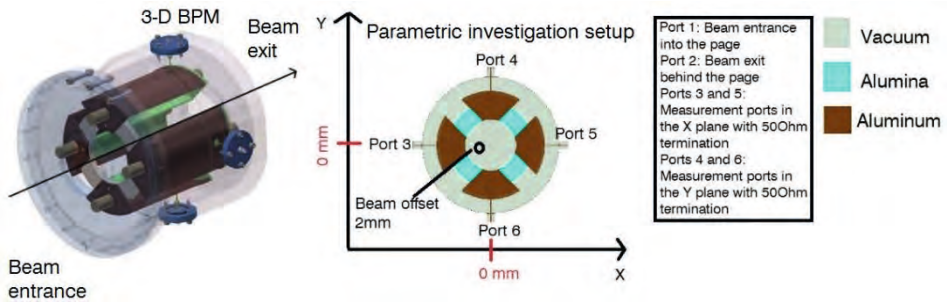

Figure 4.5: 3-dimensional view of the BPM and the sketch of the parametric investigation setup.

- *The gap between individual cavities (Inter-cavity gap)*

The gap between the four LC cavities, called an inter-cavity gap, is investigated and its findings are summarized in Table 4.3.

Table 4.3: Summary of the parametric investigation. The loaded Quality factors (both TM_{010} mode and TM_{110} mode) are evaluated from the S_{xx}. The S_{xy} and S_{xx} evaluated do not depend on the beam analog position.

Gap (mm)	**Freq$_{TM010}$ (MHz)**	**Freq$_{TM110}$ (MHz)**	**ΔFreq (MHz)**	**$Q_{L,TM010}$**	**$Q_{L,TM110}$**	**$\Delta S_{2mm-0mm}$ (dB)**
20	118.2	142.8	24.6	43	86	3
40	127.1	145.4	18.3	37	47	2
60	136.6	149.7	13.1	28	23	1

Increasing the inter-cavity gap increases the TM_{010} and the TM_{110} mode resonance frequencies since the cross-sectional area of the capacitive region in the LC cavities is reduced, as shown in Figure 4.6. The TM_{110} mode frequency is not shifted by the same extent as of the TM_{010} mode, probably due to the relatively stronger influence of the stray capacitance (i.e., includes the capacitance between the floating cavities (with each other) and the ground cylinder) on the TM_{110} mode lumped element equivalent circuit. Moreover, increasing the inter-cavity gap decreases the azimuthal coverage of the LC cavities, due to which the loaded quality factors of both the TM modes ($Q_{L,TM010}$ and $Q_{L,TM110}$) are reduced. This is because of increased power dissipation on the surface area of the ground cylinder that is now available due to the decreased azimuthal coverage of the floating cavities. Altogether, the combination of reduced frequency separation, ΔF_{req} and the decrease in the $Q_{L,TM010}$ and $Q_{L,TM110}$ results in lowering the signal sensitivity, $\Delta S_{2mm-0mm}$, (dotted lines in figures) for a given offset when increasing the inter-cavity gap.

The inter-cavity gap is chosen as a **40 mm gap** for the BPM prototype, as it offers freedom for TM_{110} mode frequency offsets without too much compromise on the quality factor and the beam-pickup coupling.

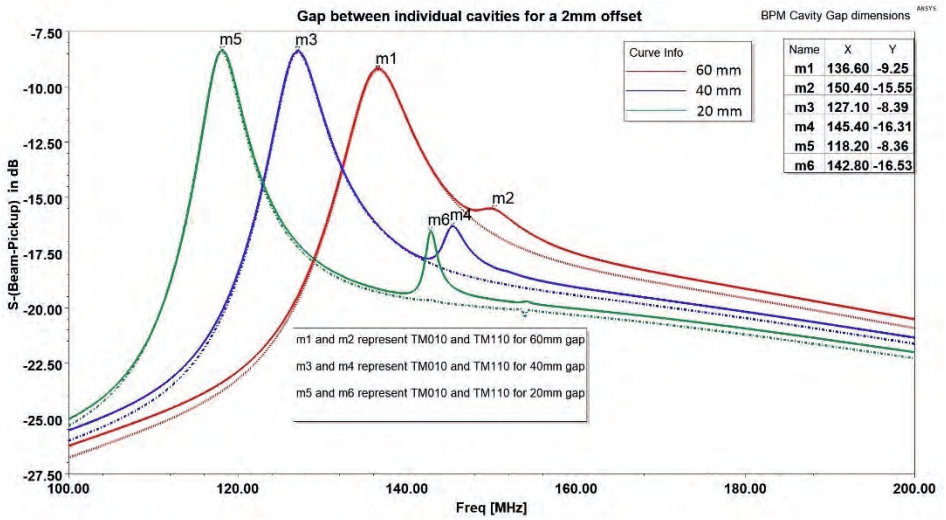

Figure 4.6: Parametric investigation of the gap between floating cavities plotted as $S_{(beam\text{-}pickup)}$ over frequency span 100-200 MHz. Shown are the coupling coefficients at 2mm beam analog offset position for three different scenarios: 20 mm, 40 mm, and 60 mm gap between floating cavities. The dotted lines represent the S-parameter curve for the center position.

- *The gap between Cavities and Grounded cylinder (Intra-cavity gap)*

The effect of the gap between the LC cavities and the ground cylinder, called an intra-cavity gap, is investigated and its findings are summarized in Table 4.4. This investigation is performed for the inter-cavity gap dimension fixed at 40 mm.

Table 4.4: Summary of the parametric investigation. The loaded Quality factors (both TM_{010} mode and TM_{110} mode) are evaluated from the S_{xx}. The S_{xy} and S_{xx} evaluated do not depend on the beam analog position.

Gap (mm)	**$Freq_{TM010}$ (MHz)**	**$Freq_{TM110}$ (MHz)**	**$\Delta Freq$ (MHz)**	**$Q_{L,TM010}$**	**$Q_{L,TM110}$**	**$\Delta S_{2mm-0mm}$ (dB)**
15	127.4	147.2	19.8	31.5	45	2.3
25	127.1	145.5	18.3	37	47	2.0
35	127.1	144.4	16.3	42	46	2.0

The intra-cavity gap does not strongly affect the TM_{010} mode resonance frequency as the stray capacitance between the cavities and the ground cylinder does not affect the lumped element equivalent of the TM_{010} mode. However, the TM_{110} mode resonance frequency is affected due to a stronger influence of the stray capacitance on the TM_{110} mode lumped element equivalent. Nevertheless, the

intra-cavity gap is considered a critical parameter, as it plays a role on the beam-pickup coupling without affecting the loaded quality factors of both the TM modes ($Q_{L,TM010}$ and $Q_{L,TM110}$) drastically. Also, the signal sensitivity, $\Delta S_{2mm-0mm}$, is nearly independent of the intra-cavity gap. Figure 4.7 shows the results of the parametric investigation of the intra-cavity gap for an inter-cavity gap of 40 mm.

The intra-cavity gap = **25 mm** is chosen, which corresponds to a ground cylinder radius of 120 mm as this provides a relatively high loaded quality factor of both the modes, a good amount of frequency separation between them, and a smaller transverse size of the cavity BPM.

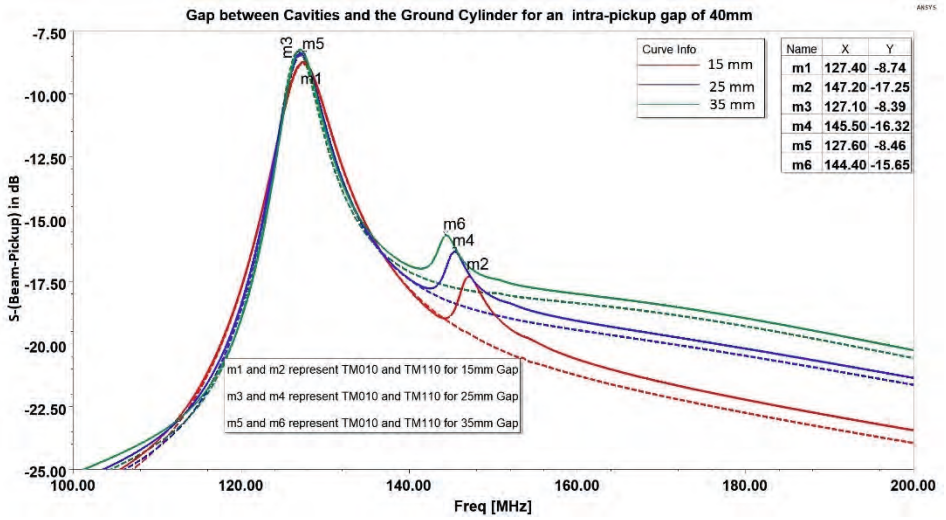

Figure 4.7: Parametric investigation of gap changes between floating cavities and the grounded cylinder on plotted as $S_{(beam-pickup)}$ over frequency span 100-200 MHz. Shown are beam-cavity 3 coupling for three different gap dimensions: 15mm, 25mm, and 35mm. The dotted lines represent the S-parameter curve for the center position.

- *Dielectric width and thickness*

The dielectric dimension is defined by the thickness in the beam direction and width as the difference between inner and outer radial dimensions. The investigation results of both the dielectric width and the thickness are summarised in Table 4.5 and Table 4.6. These parameters are investigated for an intra-cavity gap = 25 mm and inter-cavity gap = 40 mm. The dielectric width is varied by changing the outer radius of the ring for a fixed inner radius. The inner radius is not the variable parameter of the dielectric width as it could block the beam

passage area (i.e., the cross-sectional area of the beam pipe). The inner radius of the ring is fixed at 90 mm.

Table 4.5: Summary of the parametric investigation. The loaded Quality factors (both TM_{010} mode and TM_{110} mode) are evaluated from the S_{xx}. The S_{xy} and S_{xx} evaluated do not depend on the beam analog position.

Width (mm)	**Freq$_{TM010}$ (MHz)**	**Freq$_{TM110}$ (MHz)**	**ΔFreq (MHz)**	**$Q_{L,TM010}$**	**$Q_{L,TM110}$**	**$\Delta S_{2mm-0mm}$ (dB)**
26	133.1	152.2	19.1	33	45.3	2.0
28	128.4	146.9	18.5	36	46.6	1.8
30	123.8	141.6	17.8	40	48.7	1.6

The dielectric width and thickness are considered the tuning parameters for the BPM's mode frequencies. For a given thickness, increasing the dielectric width reduces both the mode frequencies by nearly the same extent without affecting the $S_{(beam\text{-}pickup)}$ at the TM_{010} mode resonance frequency. The $S_{(beam\text{-}pickup)}$ at the TM_{110} mode resonance frequency reduces, which is in agreement with Eq (4.10) due to an increase in the effective gap radius.

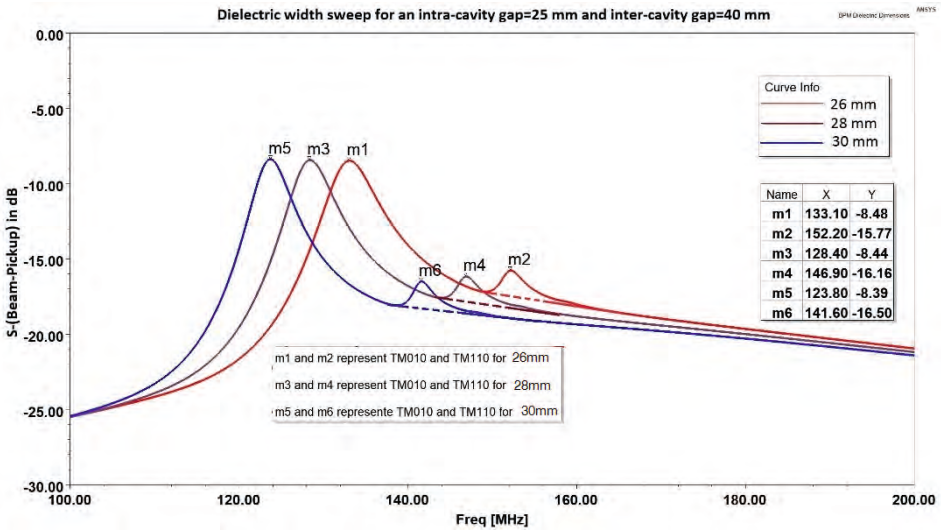

Figure 4.8: Parametric investigation of the BPM model as a function of dielectric width for an intra-cavity gap=25 mm and an inter-cavity gap=40 mm. Provided are three different width dimensions: 26 mm, 28 mm, and 30 mm. The dotted lines represent the S-parameter curve for the center position.

Table 4.6: Summary of the parametric investigation. The loaded Quality factors (both TM_{010} mode and TM_{110} mode) are evaluated from the S_{xx}. The S_{xy} and S_{xx} evaluated do not depend on the beam analog position.

Thickness (mm)	**$Freq_{TM010}$ (MHz)**	**$Freq_{TM110}$ (MHz)**	**ΔFreq (MHz)**	**$Q_{L,TM010}$**	**$Q_{L,TM110}$**	**$\Delta S_{2mm-0mm}$ (dB)**
10	127.1	145.4	18.3	37	47	2.1
12.5	139.3	158.9	19.6	29	47.5	1.9
15	150.3	170.7	20.4	25	50.5	1.9

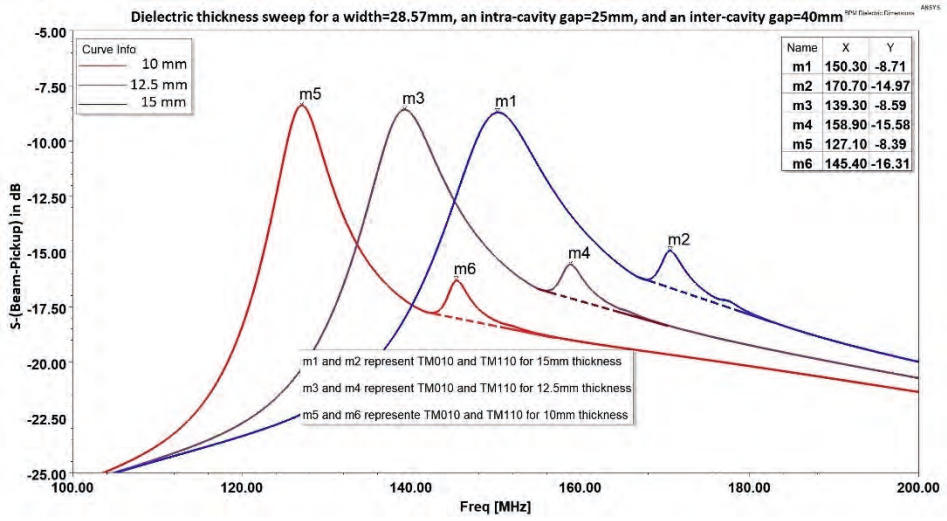

Figure 4.9: Parametric investigation of the BPM model as a function of dielectric thickness with other dimensions held constant. Provided are three different width dimensions: 10 mm, 12.5 mm, and 15 mm. The dotted lines represent the S-parameter curve for the center position.

On the contrary, for a given width, increasing the thickness increases both the mode frequencies by the same extent. The $S_{(beam-pickup)}$ of the TM_{110} mode increases with increasing dielectric thickness, which is in agreement with Eq (4.10). Moreover, changing the dielectric width or thickness does not strongly affect the loaded quality factors of both the modes and the position sensitivity of the TM_{110} mode. These behaviors are clearly seen in Figure 4.8 and in Figure 4.9.

For the alumina ring, dielectric width of **28.57 mm** is chosen for a dielectric thickness of **10 mm** for the BPM prototype. These dimensions ensure the TM_{110} mode resonance frequency to be close to 145.7 MHz.

- *Pickup position*

The effect of the pickup position on the system characteristics is summarized in Table 4.7. These investigations are performed for the selected dimensions of the intra- and inter-cavity gap and the dielectric width and thickness.

Table 4.7: Summary of the parametric investigation. The loaded Quality factors (both TM_{010} mode and TM_{110} mode) are evaluated from the S_{xx}. The S_{xy} and S_{xx} evaluated do not depend on the beam analog position.

Loop position (mm)	$Freq_{TM010}$ (MHz)	$Freq_{TM110}$ (MHz)	$\Delta Freq$ (MHz)	$Q_{L,TM010}$	$Q_{L,TM110}$	$\Delta S_{2mm-0mm}$ (dB)
20	127.7	145.1	17.4	58	173	4.1
30	127.1	145.4	18.3	37	47	2.1
40	126.2	145.9	19.7	27.7	16.8	1.3

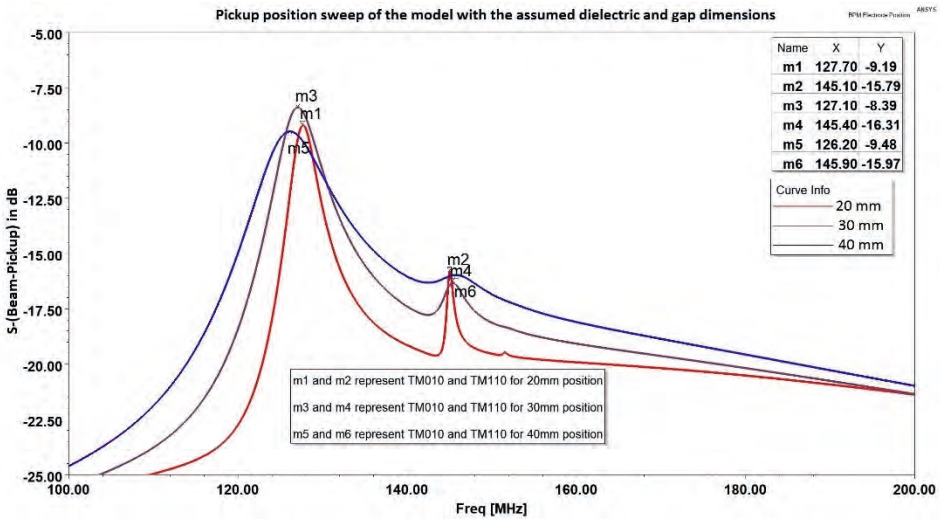

Figure 4.10: Parametric investigation of the BPM model as a function of loop position (pickup) for the previously confirmed dimensional parameters: dielectric dimensions and inter/intra-cavity gaps. Provided are three different pickup positions: 20mm, 30mm, and 40mm.

The pickup position has minimal influence on both the TM_{010} and TM_{110} mode resonance frequencies and is probably due to small changes in the loop inductance (proportional to loop area) as a function of its position. The $S_{(beam-pickup)}$ of the TM_{010} mode in Figure 4.10 increases with pickup height up to 30 mm before it is reduced for 40 mm position. This is probably due to excessive coupling compared

to the critical coupling limit. The signal sensitivity, given by $\Delta S_{2mm\text{-}0mm}$, decreases with increasing pickup height. This is due to the reduced amplitude of the TM_{010} mode at the TM110 mode frequency for lower pickup height, which facilitates larger signal sensitivity. The pickup position is chosen as 30 mm.

All the above parameters selected for the BPM prototype construction take into consideration the relaxation of machining and assembly errors. For instance, a pickup position of 20 mm will provide better signal sensitivity but due to the higher loaded quality factor, the demand on the symmetry of the model becomes more stringent. Since the construction of the BPM with perfect symmetry is not feasible, a reduction of the loaded quality factor is accepted. The symmetry of the BPM prototype is defined by the overall tolerance (machining and assembly) in linear position up to 0.05 mm and in rotational up to 0.1 degrees.

4.4 Final BPM model and simulation results for position offsets

In the parametric investigation (previous subsections), we have studied the influence of certain important geometric parameters on the characteristics of both the TM_{010} and the TM_{110} modes. The mechanical dimensions of the BPM prototype whose TM_{110} mode excitation exists at 145.7 MHz are as shown in Figure 4.11.

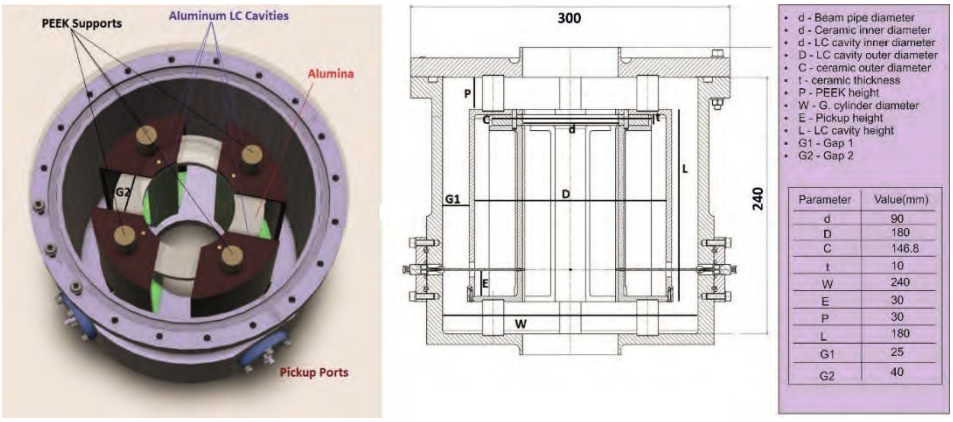

Parameter	Value(mm)
d	90
D	180
C	146.8
t	10
W	240
E	30
P	30
L	180
G1	25
G2	40

Figure 4.11: Cut plane of the BPM prototype derived from HFSS simulation. Marked are the relevant dimensions of the prototype.

4.4.1 S-transmission for position offsets

A simulation estimate of the beam position-induced signal at multiple beam offsets is provided by the Driven modal solution at: 2 mm, 5 mm, 10 mm, and 15 mm along with the center position (0 mm). The position-offset simulation is

performed only for offsets in the X-axis. Due to the symmetry of the TM_{110} mode, the $S_{(beam\text{-}pickup)}$ behavior of the Y plane cavities is the same for translation of the beam along the Y-axis. Moreover, for an arbitrary (X, Y) position, the pickup response is the sum of both the horizontal and vertical polarization because of linear superposition of their fields. In Figure 4.12, the $S_{(beam\text{-}pickup)}$ behavior of both the X and Y plane cavities for 2 mm displaced beam in the X-axis from the center towards cavity 3 (reference Figure 4.5) is displayed. Since the Y coordinate is zero, the $S_{(beam\text{-}pickup)}$ for the Y-plane cavities is representative of the center position and corresponds to the TM_{010} mode amplitude at the TM_{110} mode resonance frequency.

Figure 4.12 represents the S-transmission plot for both X plane cavities with a span of 100 MHz for a 2 mm beam offset in the X-axis. The TM_{010} mode resonance frequency of the BPM prototype is at 127.1 MHz and the TM_{110} mode resonance frequency is at 145.7 MHz. For a given displacement towards cavity 3, the polarity effect as observable in Figure 4.3 (top figure) determines the nature of the $S_{(beam\text{-}pickup)}$ plot of the X plane cavities as maximum (marker m1) and minimum (marker m2).

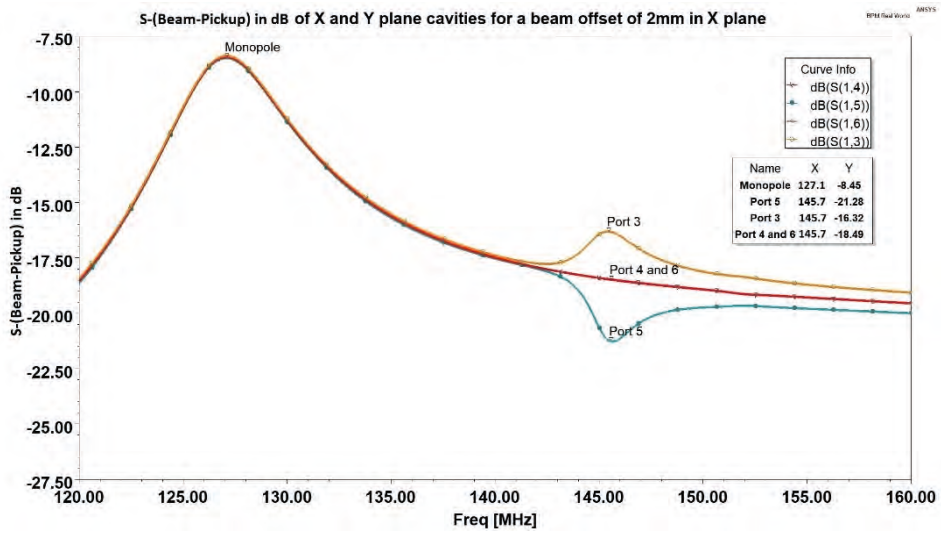

Figure 4.12: S-transmission for X (ports 3 and 5) and Y (ports 4 and 6) plane cavities for a beam offset of 2 mm in the X plane. Ports 1 and 2 are the beam entrance and exit ports (Figure 4.5). Markers (Port 3 and 5) represent the beam-pickup coupling coefficient of the X plane cavities whose TM_{110} mode is excited and is shown as maximum and minimum of the S-plots. Markers (Port 4 and 6) represent TM_{010} mode resonance frequency and TM_{010} mode tail at the TM_{110} mode resonance frequency along with their beam-pickup coupling coefficients.

For increasing beam displacement towards the cavity (port 3) in the X-axis, the $S_{(beam\text{-}pickup)}$ coefficient (maximum) at the TM_{110} mode frequency increases with no shift in its peak frequency, as shown in Figure 4.13. This is due to similar curl orientations for the cavity with measurement port 3 as indicated by the smaller relative phase difference between the TM_{010} and the TM_{110} modes in Figure 4.14. However, for the cavity (port 5), with increasing beam displacement away from the center, the minimum of the $S_{(beam\text{-}pickup)}$ shifts in frequency since there is frequency dependency of both the amplitude and phase of the TM_{010} and the TM_{110} mode with respect to the drive signal. This is due to opposite curl orientations of the induced magnetic fields between the TM_{010} and TM_{110} modes, as discussed in 4.2.1. For a sizeable beam offset such as 15 mm towards cavity with port 3, the $S_{(beam\text{-}pickup)}$ of the cavity with port 5 soars above the zero position $S_{(beam\text{-}pickup)}$ coefficient. This is a result of a stronger TM_{110} mode magnitude than the TM_{010} mode magnitude at the TM_{110} mode resonance frequency.

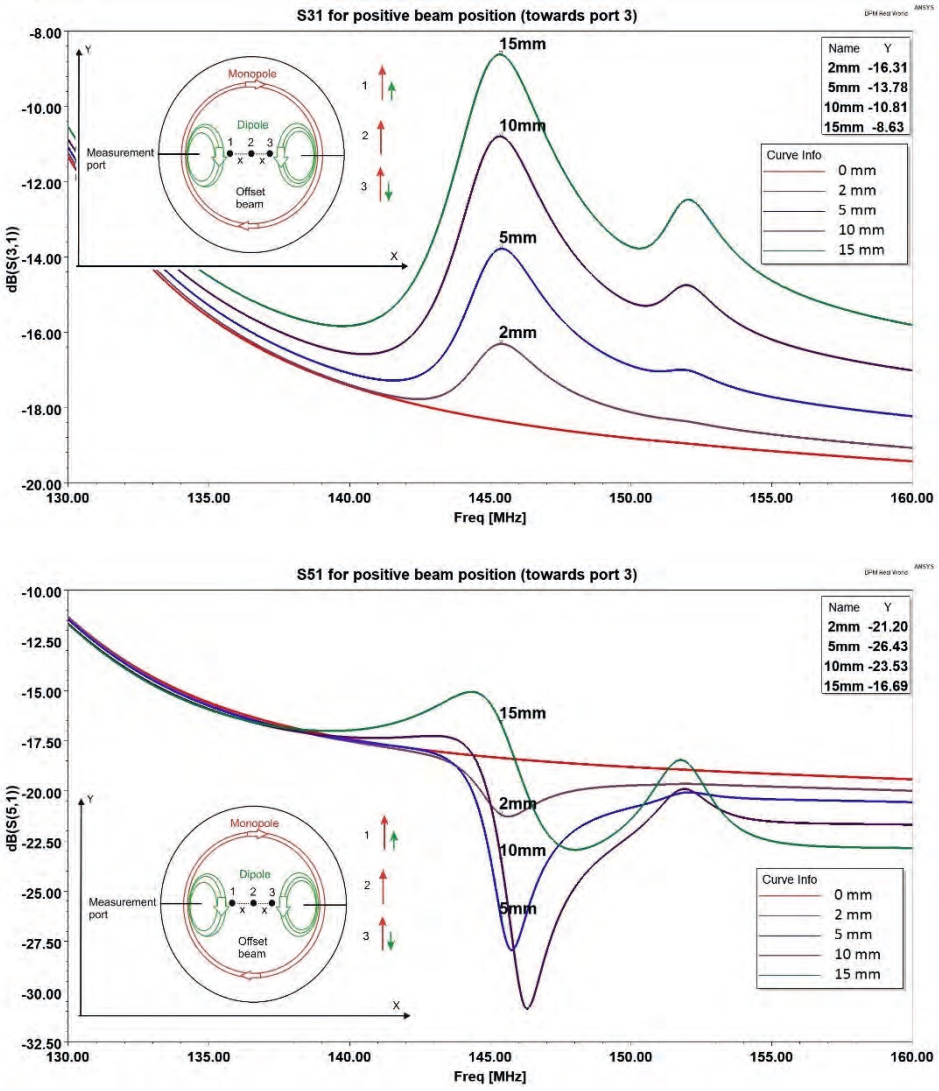

Figure 4.13: S31 (top) and S51 (bottom) transmission plots as the beam traverses towards cavity with port 3. The red line represents the center beam position indicative of scenario 2 in the fragmented image shown at the bottom left. S-transmission behavior of the cavity with port 3 is representative of scenario 1 in the fragmented image. S-transmission behavior of the cavity with port 5 is a representation of scenario 3 in the fragmented image. At displacements larger than 5 mm, another higher-order mode (i.e., TM_{210} mode) is excited at 152.5 MHz.

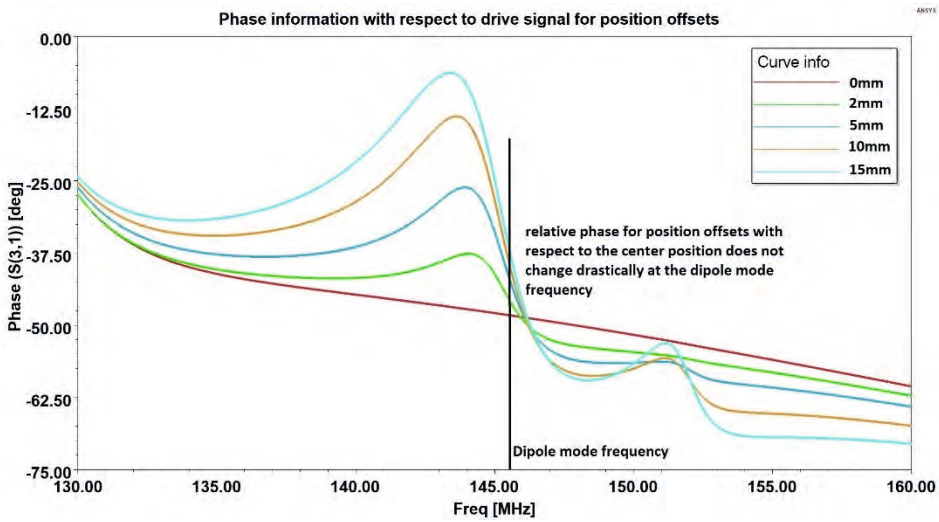

Figure 4.14: Phase plot of the measurement port 3 with respect to beam entrance port 1 for position offsets. The relative phase between the center position (TM_{010} mode phase at TM_{110} mode frequency) and the position offsets (TM_{110} mode phase) does not change drastically. Thus, the superposition of the modes does not shift the peak frequency in Figure 4.13 (top).

For beam displacements larger than 5 mm, another higher-order transverse magnetic mode is excited at 152.5 MHz. The higher-order mode is categorized as the TM_{210} mode (confirmed by simulation) since it has two full period variations of the azimuthal field components and one zero-crossing of the longitudinal field components. This indicates that for beam offsets larger than 5mm, we might face the effects of mode interference also from TM_{210} mode. This can be determined in a calibration procedure, however.

For the measurement chain, the position signal level from the BPM prototype will be low and will have to be bandpass filtered to get rid of the fundamental frequency, i.e., 72.85 MHz, and its higher harmonics (≥ 3). For determining the beam displacement and its sign, we have to consider the combination of all the measurement ports to determine in which quadrant the beam belongs. The simulation results for position offsets of 2 mm, 5 mm, 10 mm, and 15 mm is evaluated as per Eq (4.12) [15] and are summarized in Table 4.8.

$Z_{tr,i}$ is the transfer impedance of a given pickup (i.e., measurement port) and could be used to evaluate the position signal from the BPM prototype.

$$Z_{tr,i} = \frac{S_{1i}}{S_{12}} \sqrt{Z_o Z_c} \tag{4.12}$$

where,

- S_{12} is the S-transmission between beam entrance and beam exit port;
- S_{1i} is the transmission coefficient of a port (3,4,5 or 6) for a given offset
- Z_o is the port impedance of 50 Ω and Z_c is the characteristic impedance of the transmission line the beam analog forms with the cavity = 366 Ω.

NOTE: The S-transmission coefficients for the position offsets are provided in the Appendix.

Table 4.8: Summary of simulation results for displacements towards cavity 3. The pickup voltage is evaluated for a 50 Ω impedance system.

Position(mm)	S31 (dB)	Pickup Voltage (nV)
0	-18.45	16.2
2	-16.31	20.5
5	-13.78	27.5
10	-10.81	38.7
15	-8.63	49.7

4.4.2 Crosstalk (XX and XY)

For the crosstalk study of the BPM, the Driven modal analysis is performed in the absence of a beam analog. The nature of the XX and the XY crosstalk can be clearly seen in Figure 4.15.

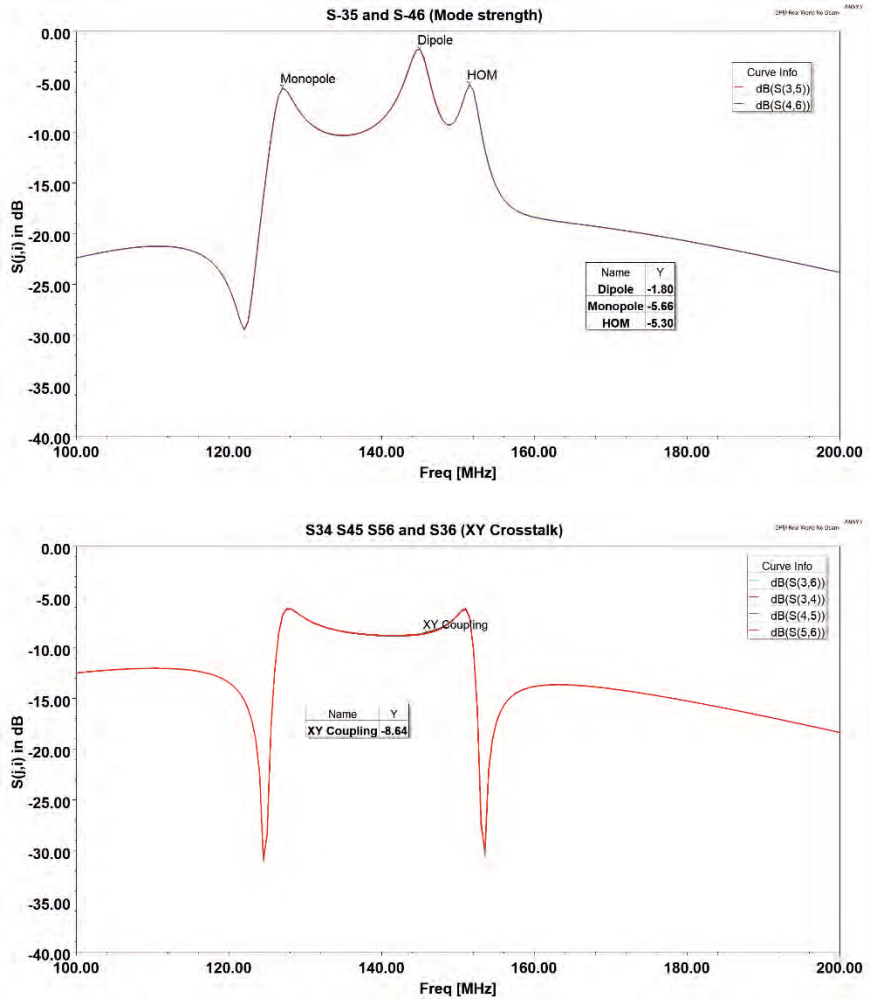

Figure 4.15: XX crosstalk (Mode strength) and XY crosstalk evaluated from the s-transmission plots in the absence of the beam analog. In the top plot, TM_{010} mode resonance frequency is at 127.1MHz, TM_{110} mode resonance frequency at 145.7MHz and the TM_{210} mode (indicated as Higher Order Mode (HOM)) resonance frequency is at 152.5 MHz. In the bottom plot, the XY coupling is representative of the horizontal-vertical crosstalk. The marker values are in dB.

The frequency-dependent XX (or YY) crosstalk at the TM_{110} mode is especially high. This could affect the position sensitivity and the resolution along the corresponding axis, as it would be in a capacitive monitor since the signal generation is dominated by this crosstalk. However, in a cavity BPM, for a given offset in the horizontal (or vertical direction), the horizontal (or vertical) TM_{110} mode excitation is localized mostly between the two in-plane cavities but with

opposite polarity. For a cavity in which the TM_{110} has opposite polarity with respect to the stronger TM_{010} mode, the position information could be lost due to this opposition. This effect could be minimized by having a relatively stronger in-plane crosstalk at the TM_{110} mode frequency compared to the crosstalk at the TM_{010} mode frequency. However, this is achieved at the expense of position sensitivity and resolution. The in-plane crosstalk is assumed to not affect the position resolution demand for PROSCAN, which is 0.5 mm.

What is greatly detrimental for the cavity BPM would be strong crosstalk between the horizontal and the vertical TM_{110} mode, represented by the XY crosstalk. This would create a parasitic excitation of the TM_{110} mode in the Y-(X-) direction for a beam position offset X- (Y-) direction. This would seriously compromise reduce the capability of the cavity BPM to measure beam position offset.

Limiting the crosstalk between the adjacent pickups is thus important in the design of BPMs. This is traditionally achieved either by increasing the spacing between the adjacent pickups or with a more complicated geometry such as guard rings. The choice of a guard ring is not considered since we do not want to add more complexity to the already complex design of the cavity BPM.

Source of crosstalk: Shorted Stripline

Strong crosstalk arises mostly from capacitive coupling between X- and Y-cavities. For a conventional pillbox, the crosstalk is only between the pickups, i.e., inductive loops, whereas, for our BPM, the presence of four floating cavities represents an analogy of four capacitive electrodes. However, the electrodes are constructed as LC resonators (geometrically), which causes the BPM system as a whole to behave as a combination of resonators and capacitive probe. Specifically, the four LC resonators also represent themselves as stripline electrodes with a short termination at the base of the LC cavity and a load termination with 50 Ω (at measurement ports), which is similar to a shorted stripline BPM [16]. The combination of shorted stripline and resonating behavior of the BPM prototype is clearly seen in the simulation results shown in Figure 4.16.

Depending on the orientation of the BPM, it couples stronger to the beam when the beam enters such that it sees the cavity gap first, as shown in Figure 4.16. When the beam enters from the opposite end, the pickup couples to the beam relatively weaker. This behavior is a clear indication of shorted stripline behavior, which is generally used as a directional coupler. For a pillbox cavity, this behavior is non-existent.

Thus, the source of stronger crosstalk between adjacent pickups arises from the capacitive coupling (between the cavities) along with the mode interference caused by the smaller loaded quality factor and frequency separation.

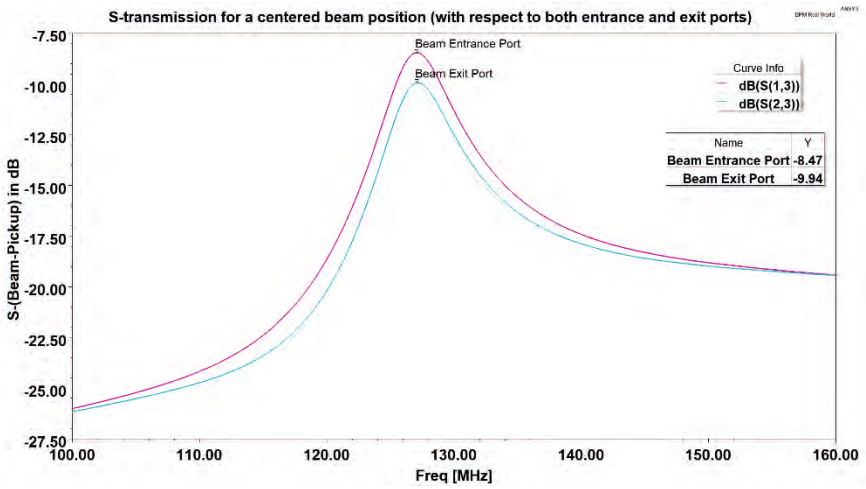

Figure 4.16: S-transmission of the BPM system (cavity 3) with respect to beam entrance and exit ports (i.e., S13 and S23) at the TM_{010} mode resonance frequency. The S-transmission coefficient differs by approx. 1.5dB. The simulation is performed with a beam analog presence. Marker values are in dB.

Comparison with pillbox equivalent

The XX (or YY) crosstalk of the BPM is approximately 15% lower than that of a pillbox equivalent. However, the XY crosstalk of the BPM is threefold higher than the pillbox equivalent. Even though a pillbox system seems to offer much better XY isolation, for measurement with 1 nA, the absolute level of the signal for small position offsets is much closer to the thermal noise in a pillbox cavity. For instance, a 10 mm offset position in a pillbox BPM is expected to deliver a pickup voltage at approximately 3.5 nV. For the BPM prototype, the pickup is expected to deliver a ten times higher signal for the same offset at approximately 39 nV. These signal levels are when the second harmonic amplitude from the bunch is 1 nA. For a bunch length of 2 ns (at the degrader exit), the second harmonic amplitude is approximately 25% of the average beam current.

From the above observation, a cavity BPM built as a combination of four floating cavities offers a higher signal level for a given position offset and higher position sensitivity compared to a conventional pillbox cavity. Another advantage it offers is the compactness of the system and directivity.

4.4.3 Cavity asymmetries

The cavity asymmetry study is performed on the BPM model to quantify its influence on cavity signal amplitude and on the TM_{110} mode resonance frequency. The cavity asymmetries that are considered for the study include:

- Cavity position error
- Dielectric position error
- Dielectric properties error, ε_r
- Cavity rotation: Roll, Pitch, and Yaw

The asymmetry studies are performed on a single cavity within the model. The remaining cavities are not changed (i.e., no offsets induced). The left translation is indicative of negative displacements and the right translation of positive displacements. Rotational offsets are set in units of degree. The influence of these asymmetries on the TM_{110} mode resonance frequency and the $S_{(beam\text{-}pickup)}$ coefficient is reported as these are the primary parameters of concern.

Cavity position error

The cavity (X1) marked with the double arrow (red) is displaced to both left and right by 0.5 mm with respect to its optimal design position, i.e., the reference position. The results shown in Figure 4.17 are of the X2 cavity for a translation of the X1 cavity.

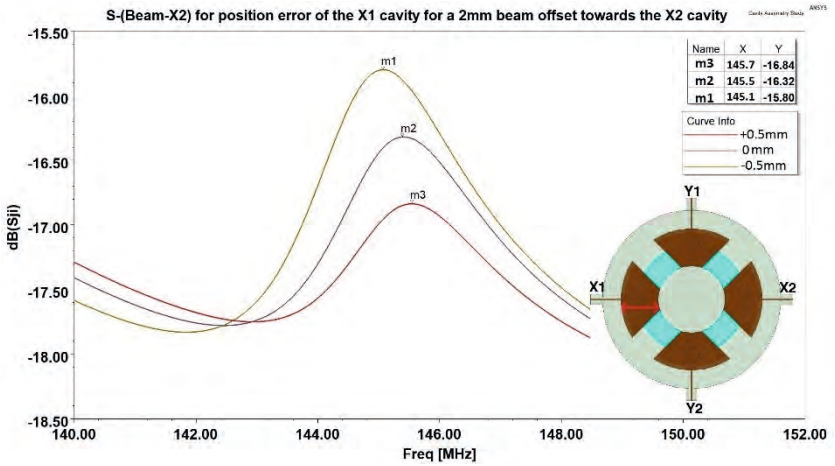

Figure 4.17: S_{ji} of the cavity X2 (beam offset of 2mm towards the right cavity) for translation errors of the opposite cavity, i.e., X1. The results are plotted for displacements of X1: -0.5mm; 0 mm; +0.5 mm. Port *j* represents the X2 cavity port and port *i* represents the beam entrance (into the page). Color reference for the fragmented image can be found in Figure 4.5.

The TM_{110} mode resonance frequency is shifted by approximately 600 kHz for a translation of 1 mm of a single cavity. In addition, the $S_{(beam\text{-}pickup)}$ coefficient of the X2 cavity reduces overall by 1 dB as the X1 cavity is moved from left to right by an overall translation of 1 mm. In other words, a translation error of a single cavity by 1mm (±0.5 mm from the center) could result in a variation of $S_{(beam\text{-}pickup)}$ by approximately 1dB. With respect to the TM_{010} mode amplitude at the TM_{110} mode frequency, the signal level of the X2 cavity is approximately 5.8 nV higher for the - 0.5 mm displacement of the X1 cavity. Compared to the +0.5 mm displacement of the X1 cavity, the X2 cavity signal is 3.3 nV higher than the zero position. This increase in signal level of the X2 cavity by 2.5 nV is compensated by the decrease in the signal level of the X1 cavity and corresponds to a difference in position information by approximately 1.1 mm. There is little to marginal impact, i.e., 0.3% reduction in the XX (YY) crosstalk and 2.5% reduction in the XY crosstalk. The loaded quality factor is not influenced by the position error of a single cavity in the BPM model.

Dielectric position error

In Figure 4.18, the double arrow (red) indicates the displacement direction of the dielectric in the simulation. The dielectric (colored blue) is displaced by 0.5 mm to the right and 0.5 mm to the left from its reference position, i.e., its center position.

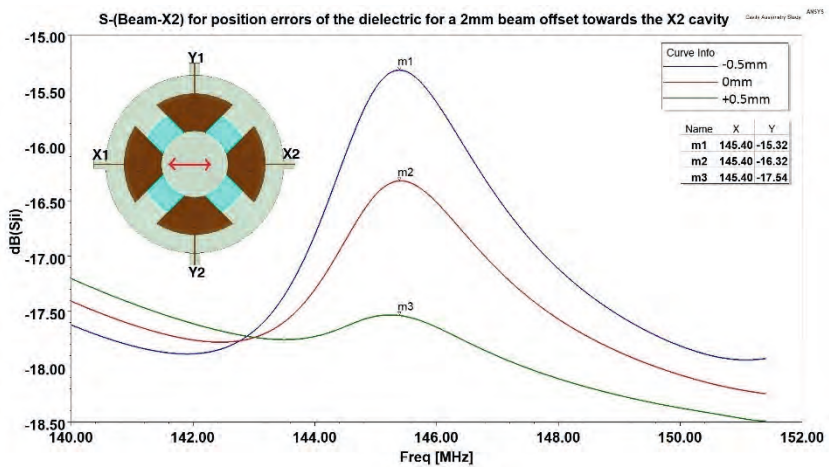

Figure 4.18: S_{ji} of the cavity X2 (for a beam offset of 2 mm towards the right cavity) for translation errors of the dielectric. The results are plotted for displacements of the dielectric: -0.5mm; 0 mm; +0.5 mm. The S_{ji} is plotted for the X2 cavity. Port *j* represents the X2 cavity port and port *i* represents the beam entrance (into the page). Color reference for the fragmented image can be found in Figure 4.5.

From Figure 4.18, we clearly see that the position offset of the dielectric has no clear influence on the TM_{110} mode resonance frequency; however, the $S_{(beam\text{-}pickup)}$ of the X2 cavity is increased by approximately 2 dB for a total displacement of 1 mm of the dielectric (+0.5 mm to -0.5 mm). With respect to the TM_{010} mode amplitude, the signal level of the X2 cavity is 7 nV higher when the dielectric is off from its reference position by -0.5 mm and is only 1.8 nV higher when the dielectric is off by +0.5 mm with respect to its reference position. This corresponds to the difference in the signal level of the X2 cavity by approximately 5.2 nV and an overall difference (between -0.5 mm and +0.5 mm model) of 2.4 mm in the position information. The volume of the dielectric that these fields have to propagate through determines the amount of beam-induced fields that terminate on the conducting walls. Thus, for identical signal-coupling by the LC cavities for a given offset, the symmetric position of the dielectric with respect to the floating LC cavities is essential. In other words, by inducing an offset in the dielectric position, the position sensitivity of the LC cavities is altered individually without noticeable changes in the loaded quality factor of the individual cavities. The XX (or YY) crosstalk is not affected by the dielectric position error; however, the crosstalk between X2-Y2 (/Y1) is increased by 7% approximately when the dielectric is displaced 0.5 mm towards X2 and reduces by 7% for a dielectric position error of 0.5 mm in the opposite direction. Due to the above influence on the crosstalk, the Y2 cavity shows a beam position offset of 0.3 mm towards it when in reality, the Y coordinate is actually zero.

Cavity rotation

The X2 cavity (reference Figure 4.18) is rotated by 1 degree with respect to the beam axis (longitudinal axis). The other LC cavities, alumina ceramic and the PEEK supports are at their symmetric position. With the rotation of a single cavity (X2), the beam-pickup coupling coefficient of the X2 cavity is increased by 0.1 dB, which corresponds to an increase in the signal information by 0.5 nV (beam position error of 0.15 mm). In addition, the Y-axis cavities give a position offset of 0.4 mm due to the 1-degree rotation of the X2 cavity, instead of a zero Y coordinate. This is a consequence of the combination of amplified crosstalk (25% higher) between the X2-Y1, X1-Y2 cavities and diminished crosstalk between X1-Y1 and X2-Y2 cavities (25% lower). There was no frequency shift of the cavities observed in the simulation studies.

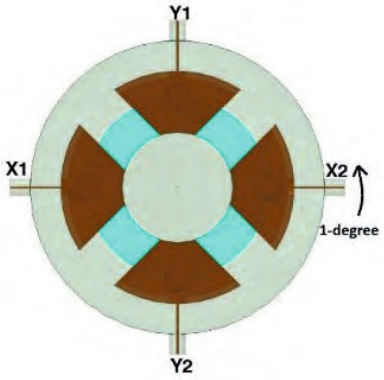

Figure 4.19: X2 cavity rotated 1 degree towards Y1 cavity. The other components of the BPM: X1, Y1, Y2 cavities, the alumina ceramic and the peek rings are in their symmetrical (default position). Color reference for the image can be found in Figure 4.5.

The pitch and yaw rotational offsets, defined by the rotation of the cavity with respect to the beam's transverse and normal axis, does not affect the $S_{(beam\text{-}pickup)}$ coefficients and the crosstalk. The yaw asymmetry of the X2 cavity by 1 degree towards the center increases the TM_{110} mode resonance frequency by 100 kHz, which could be due to a reduction in the equivalent reentrant gap radius.

4.5 Analytical evaluation

We deduce from Eq (4.1), that the resonance frequency of the TM_{110} mode for our prototype is a function of R_{res}. From the geometry of the resonator BPM that has been designed in HFSS, we assume the E- field configurations of the TM_{110} mode are sustained mostly within the R_{res}= 90 mm and in the capacitive gap of l = 10 mm in the longitudinal direction, which is filled with the dielectric.

For the analytical evaluation, certain parameters are taken from the HFSS Eigenmode solutions, which includes

- Q_0 = 3082 the unloaded quality factor of the TM_{110} mode.
- δ = 6.78 μm skin-depth for aluminum at 145.7 MHz

Substituting the resonator gap length l and the gap radius R_{res} into Eq (4.8), for a transit time factor T_{tr} = 1, we get

$$\left(\frac{R}{Q_0}\right)_{110} = \frac{2\,Z_0\;l\;(J_1^{max})^2\;T_{tr}^2}{\pi\,R_{res}\;J_o^2(a_{11})\,a_{11}} \approx 130.73\;\frac{l}{R_{res}}\;T_{tr}^2 \approx 14.52\;\Omega$$

The transit time factor is nearly 1 for all the proton beam energies (238-70 MeV) as per [11].

The voltage V_{110}^{in} induced by a bunch charge q (corresponding to 1 nA beam current at the drive frequency i.e., 145.7 MHz) in the TM_{110} mode at a given displacement of $\delta x = 2.0$ mm (at $\phi = 90$), can be calculated using the Eq (4.10).

Substituting $a_{11} = 3.83$ (first zero of the first-order Bessel function), R_{res} and $J_1^{max} = 0.582$ (maximum of the first-order Bessel function) for the offset in the angle bracket term the beam-coupling coefficient is B_c=0.51. The induced voltage as per Eq for the bunch charge

$$V_{110}^{in}(\delta x)=\omega\, q \left(\frac{R}{Q}\right)_{110} \left\langle \frac{a_{11}\,\delta x}{2\, J_1^{max}\, R_{res}} \right\rangle == \frac{0.2474\,\delta x\, q\, l\, T_{tr}^2}{R_{res}^3} = 92.30 \text{ nV}$$

for $\omega = 2\pi f = 9.15\times10^8$ rad/s

From the HFSS Driven Modal solution, the loaded quality factor, Q_L, of the cavity = 46 where, $\chi = Q_o/Q_L$ is given as 66.

Substituting the derived parameters in Eq (4.11), provides expected output voltage for a 2 mm displacement as

$$V_{110}^{out}(\Delta x)=\left(\frac{R}{Q}\right)_{110} \omega\, q \sqrt{\frac{50\Omega}{Q_L}} B_c \frac{\chi}{1+\chi} = 25 \text{ nV(approx.)}$$

The order of magnitude matches with the simulation estimate (20.5 nV for 2 mm displacement). The simulation estimate being more precise will be used as a reference. These signal levels are when the second harmonic amplitude from the bunch is 1 nA. For a bunch length of 2 ns (at the degrader exit), the second harmonic amplitude is approximately 25% of the average beam current.

4.6 Conclusion

For the measurement of the beam position of a proton beam in PROSCAN beamlines, the use of a cavity resonator based on the principle of TM_{110} mode resonance is considered.

The characterization of the TM_{110} mode described in subsection 4.1.1 demonstrates the linear response of the TM_{110} mode cavity for position offsets. In a traditional cavity BPM such as a pillbox, the TM_{110} mode resonance frequency is located at a few hundreds of MHz from the TM_{010} mode resonance frequency of the cavity to ensure minimum mode interference. However, our cavity BPM has its TM_{110} mode resonance frequency (145.7 MHz) within 20 MHz from the TM_{010} mode resonance frequency (127.1 MHz). This allows to take advantage of the mode interference exploiting by the opposite polarity between the TM_{010}

mode and the TM_{110} mode to determine the sign of the beam position offset as described in subsection 4.2.1.

The Driven modal solver provided mechanical dimensions of certain important design parameters, which includes

- Gap between individual floating cavities (inter-cavity gap)
- Gap between the ground cylinder and the floating cavities (intra-cavity gap)
- Dielectric dimensions: dielectric width and thickness
- Pickup position

The above-mentioned parameters were optimized to maximize the TM_{110} signal output at 145.7 MHz for a given bunch charge and a beam position offset. The cavity BPM dimensions are as shown in Figure 4.11. The advantages of the BPM over pillbox equivalent are the higher absolute signal level for a given offset, its better position sensitivity and its compactness. The analytical evaluation is also in good agreement with the simulation results, thus giving confidence in the expected response of the BPM prototype for ultra-low proton beam currents. The slope of the linear relationship shown in Figure 4.20 gives the position sensitivity of the cavity BPM. The offset at beam position zero (0 mm) is mostly caused by the signal from the TM_{010} excitation. The next Chapter discusses the test-bench and beamline measurements of the above-designed cavity BPM.

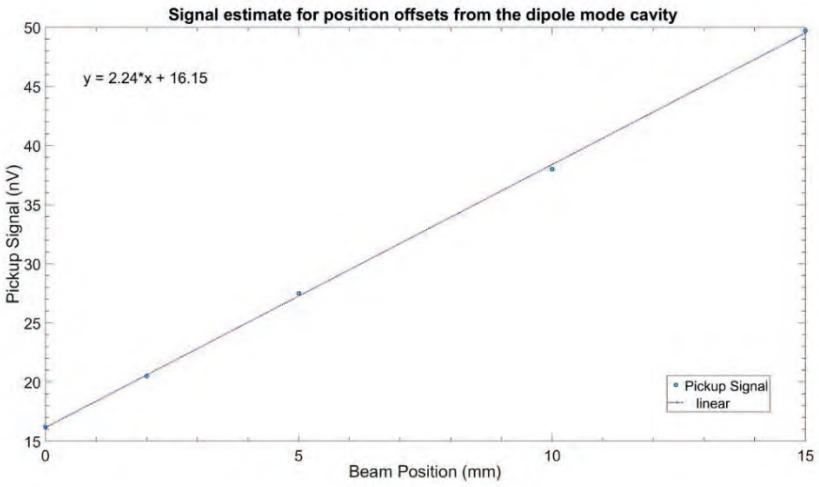

Figure 4.20: Theoretical position sensitivity of the cavity BPM estimated from simulation results

4.7 Appendix

S-parameter Transfer Matrix for beam position offsets

4TA 1: S-transmission matrix (magnitude) for simulated beam position offsets. The diagonal elements of the matrix represent reflection coefficients. The other elements represent transmission coefficients. 1 and 2 represent beam entrance and exit. 3 and 5 are for X-axis cavities. 4 and 6 are for Y-axis cavities.

Position (mm)	S-11	S-21	S-31	S-41	S-51	S-61
0	0.02	0.97	0.12	0.12	0.12	0.12
2	0.02	0.97	0.15	0.012	0.08	0.12
5	0.03	0.96	0.20	0.12	0.04	0.12
10	0.05	0.94	0.28	0.12	0.05	0.12
15	0.08	0.90	0.36	0.11	0.13	0.11

4.8 References

[1] R. E. Shafer, “Beam Position Monitoring,” *AIP Conf. Proc.*, vol. 212, pp. 26–58, 1990, doi: 10.1063/1.39710.

[2] R. Dölling, “Ionisation chambers and secondary emission monitors at the PROSCAN beam lines,” in *AIP Conference Proceedings*, 2006, vol. 868, pp. 271–280, doi: 10.1063/1.2401414.

[3] R. Lorenz, “Cavity beam position monitors,” in *AIP Conference Proceedings 451*, 1998, pp. 53–73, doi: 10.1063/1.57039.

[4] F. Gerigk, “Cavity types,” in *CAS - CERN Accelerator School : RF for accelerators*, 2010, pp. 277–298, doi: 10.5170/CERN-2011-007.277.

[5] S. Walston *et al.*, “Performance of a high resolution cavity beam position monitor system,” *Nucl. Instruments Methods Phys. Res. Sect. A Accel. Spectrometers, Detect. Assoc. Equip.*, vol. 728, pp. 53–58, 2013, doi: 10.1016/j.nima.2013.05.196.

[6] E. Jensen, “RF Cavity Design,” in *CAS - CERN Accelerator School*, 2007, no. 1, pp. 1–73, doi: 10.5170/CERN-2014-009.405.

[7] M. Viti, “Resonant Cavities as Beam Position Monitor Resonant Cavity and Beam Coupling,” no. May, pp. 1–9, 2009.

[8] U. K.Y.Ng (Fermi National Accelerator Laboratory, “Beam-Loading and Robinson’s Instability,” in *Physics of Intensity Dependent Beam Instabilities*, WORLD SCIENTIFIC, 2005, pp. 241–300.

[9] D. Lipka, “Cavity Bpm Designs , Related Electronics and Measured Performances,” in *Proceedings of DIPAC09*, 2009, pp. 280–284, [Online]. Available: dipac09.web.psi.ch.

[10] N. Pichoff, “Beam dynamics basics in RF linacs,” *CAS 2005 - Cern Accel. Sch. Small Accel. Proc.*, pp. 145–177, 2006.

[11] A. Facco, “Tutorial on low beta cavity design,” in *Proceedings of the 12th International Workshop on RF Superconductivity, Cornell University*, 2005, pp. 21–33, [Online]. Available: http://accelconf.web.cern.ch/accelconf/SRF2005/papers/sua04.pdf.

[12] C. Simon *et al.*, “Performance of a reentrant cavity beam position monitor,” *Phys. Rev. Spec. Top. - Accel. Beams*, vol. 11, no. 8, pp. 1–10, 2008, doi: 10.1103/PhysRevSTAB.11.082802.

[13] T. Nakamura, “Master Thesis Development of Beam-position Monitors with High Position Resolution,” The University of Tokyo, 2008.

[14] "Aluminum Oxide Ceramic Properties." https://www.accuratus.com/alumox.html (accessed Jan. 24, 2020).

[15] A. Gallo, A. Ghigo, F. Marcellini, M. Serio, B. Spataro, and M. Zobov, "The transverse feedback kicker," 1995. [Online]. Available: https://www.lnf.infn.it/acceleratori/dafne/NOTEDAFNE/CD/CD-5.pdf.

[16] P. Forck, P. Kowina, and D. Liakin, *CERN Accelerator School Beam Diagnostics*. CERN EUROPEAN ORGANIZATION FOR NUCLEAR RESEARCH, 2009.